EXPLORING InAs/GaAs QUANTUM DOTS FOR NEXT GENERATION SOLAR CELLS

by

William Reid

A thesis submitted to the Faculty of the University of Delaware in partial fulfillment of the requirements for the degree of Master of Materials Science and Engineering

Summer 2013

EXPLORING InAs/GaAs QUANTUM DOTS FOR

NEXT GENERATION SOLAR CELLS

by

William Reid

Approved: _____

Matthew Doty, Ph.D.
Professor in charge of thesis on behalf of the Advisory Committee

Approved: _____

David Martin, Ph.D.
Chair of the Department of Materials Science and Engineering

Approved: _____

Babatunde Ogunnaike, Ph.D.
Dean of the College of Engineering

Approved: _____

James G. Richards, Ph.D.
Vice Provost for Graduate and Professional Education

TABLE OF CONTENTS

LIST OF FIGURES

ABSTRACT

Due to the current economics surrounding energy production, it is imperative that we increase the efficiency of solar cells if we hope to lessen our dependency on fossil fuels. Current device structures waste much of the sun's energy, losing energy as heat as apposed to converting it into electricity. Quantum Dot's (QDs) unique material properties, such as tunable band gaps and discrete energy states, make them an ideal building block to engineer novel photovoltaic device structures. Three different QD based solar cell designs are discussed. The first, a quantum dot based intermediate band solar cell, is a design in which the QD's are incorporated into the band gap of an existing solar cell. In theory this allows for a two-photon process that utilizes photons that would generally be wasted in a traditional solar cell. Theory predicts that for this idea to work efficiently the quantum dots must form delocalized bands in the band gap of the solar cell. A theoretical calculation is performed to determine if this delocalized band is possible. It is determined that at least three orders of magnitude of improvement in the homogeneity of quantum dots is needed in order create a delocalized band. For this reason the likelihood of creating an efficient IBSC based on QDs is deemed to be unlikely and two other ideas are proposed.

The quantum dot cluster intermediate band idea is very similar to the IBSC, except that the requirement that the intermediate band is totally delocalized is relaxed.

It is proposed that an electron wavefunction that is delocalized over only a few quantum dots might be enough to decrease relaxation rates from the conduction band to the intermediate band and therefore may result in an improved efficiency. The second idea, photon up-conversion, electrically separates the quantum dots from the solar cells. The quantum dots are coupled to a graded potential. Two low energy photons could be used to excite electrons into the first and higher excited states of a QD and then the electron could tunnel through the triangular barrier created by the graded potential in order to recombine with the hole at an energy approximately equal to the sum of the two photons used in the excitation process.

The success of all three ideas is dependent on the device structure, including the thickness of tunneling barriers, the barrier height of tunneling barriers, and the homogeneity of quantum dots. In order to determine the optimal device structure for any of these three ideas, it is vital that we understand the effect of these device structures on the electron lifetime and charge transport dynamics. A method for examining the electron lifetime as a function of device structure using time-resolved photoluminescence is discussed.

Chapter 1

INTRODUCTION

The global demand for energy is large, over 500 Quadrillion BTU in 2009[1], and rising rapidly. One factor driving the increasing demand is the rapid growth of economies of large population centers such as India and China, whose citizens are increasingly able to afford energy intensive lifestyles that have long been considered standard in the western world. The growth in energy demand can also be attributed to the rapid increase in the use of electronic devices. This accelerated growth in energy demand is nothing new to the energy market. In the past century, spurred by public works projects such as the new deal and good old fashioned greed, America managed to go from candles and horse drawn carriages to iPhone flashlight apps and Ford Explorers. The rapid growth in demand has typically led to a market in which the most consistent and cheapest (and abundant) available option dominates. Due to their high energy density and relative availability, fossil fuels such as coal and crude oil have proved to be the cheapest option for the past century. As a result fossil fuels have dominated the energy market (providing ~70% of the electricity market and nearly all

of the transportation market in 2007).[2] Recently, however, there have been growing concerns about the connections between the burning of fossil fuels and climate change. These concerns have led to a dramatic increase in research into sustainable energy technology over the past 10 years[3]. Due to the coupling between energy and economics this research is often focused on providing an economically viable alternative to the commonly used fossil fuels.

There are currently many technologies that can provide sustainable energy, however widespread adoption of these technologies has been limited by the economics. For example, photovoltaic technology has already advanced to the point at which solar cells produce electricity more cheaply than coal fired power plants if the cost is averaged over the lifetime of a module and government subsidies for solar are included. However, the large up front capital investment required for a solar cell plant is not recovered for 10-18 years of use from cells with 15-25 year lifetimes[4]. Until the payback time is decreased significantly, major investors will continue to shy away.

The payback time for a solar cell depends on four factors: the cost of the materials and production for the device, the cost of installation, the amount of energy produced over the lifetime of the module, and the price at which the electricity can be sold. The sale price is market driven and cannot be controlled without government regulation, but history (and my electric bill) suggests it will continue to increase slowly. There are many active research programs searching for ways to decrease the cost of production and installation and/or increase the efficiency over the lifetime of solar cells. As shown in figure 1, increases in the efficiency of silicon and thin film

solar cells, which currently dominate the market, have tapered off over the past 10 to 14 years.[5] Although there continue to be small improvements due primarily to process optimization, these improvements are unlikely to result in major advances that can stimulate a disruptive change in the economic balance. Multi-junction solar cells have made steady and significant improvements, but these devices require complex fabrication and often operate effectively only under solar concentration. Consequently multi-junction solar cells are expensive and likely to remain expensive. In order to make an impact on the market and build the groundwork for a more sustainable future, significant increases in solar energy conversion efficiency without significant increases in cost are necessary. Pursuing this goal requires exploration of new sustainable energy conversion technologies.

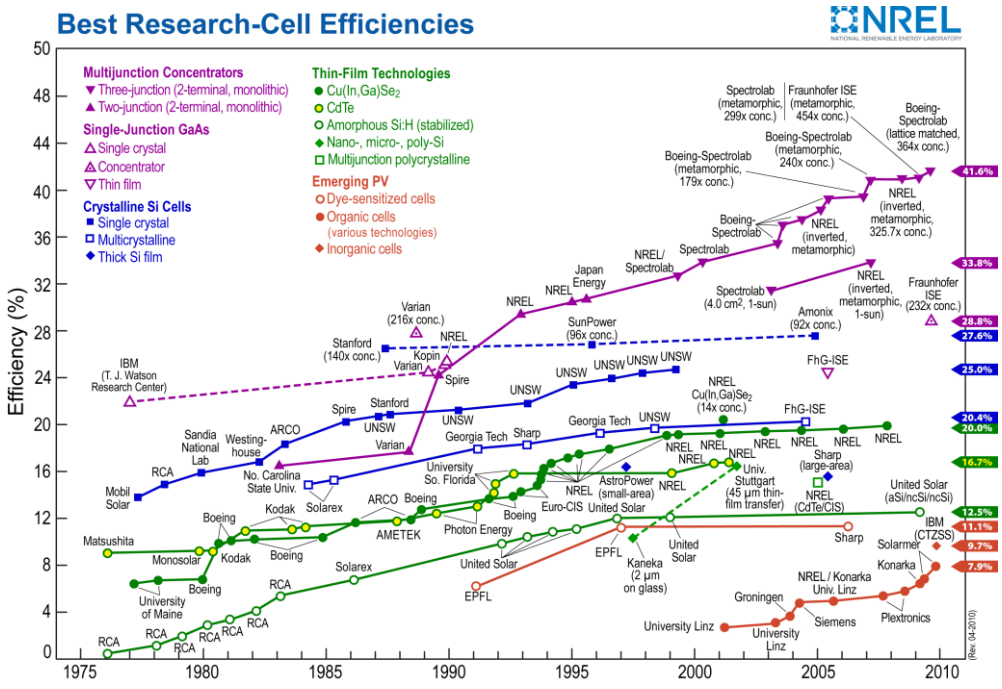

Figure 1 NREL best research cell efficiency. This shows the most efficient solar cells categorized by type from 1975 to present.

Efficiency increases in multi-junction solar cells arise from the ability to use a broader range of the solar spectrum. In traditional solar cells, photons of energy below the band gap of the material ($E_{ph}<E_g$) are not utilized because they do not have enough energy to promote a valence electron to a conduction band state. Photons of energy greater than the band gap of the material ($E_{ph}>E_g$) are not fully utilized because the photo-generated carriers relax down to the edge of the band gap before they can be extracted, wasting any additional photon energy as heat. Multi-junction solar cells combine materials tailored for different parts of the solar spectrum in order to increase the efficiency. The utilization of low energy photons does come at a price, however. By lowering the band gap of the material to increase the current (I) from low energy photons, one decreases the potential (V) of each electron, which results in diminishing power (P=IV). This results in a maximum efficiency of 40.7 for two junctions.[6] Increasing the number of junctions will lead to an increase in theoretical efficiency beyond the 40.7 When considering the unavoidable cost of processing multiple layered solar cells (typically at very high heats and vacuum) with multiple electrical connections, and when considering that current matching is a necessity to reach maximum efficiency, it is valuable to explore alternatives to use the solar spectrum more effectively.

After examining the trends in figure 1 and recognizing the importance of economics on the success of any particular PV technology, it becomes obvious that ideas not shown in figure 1 need to be explored. Intermediate band solar cells (IBSC's) have been proposed as a novel way of significantly increasing the solar cell

efficiency. In this model, a half-filled band is incorporated into the energy band gap of a conventional single junction solar cell. The incorporation of the intermediate band has been predicted to increase the solar conversion efficiency under concentrated illumination from 40.7 to 63.2 %.[7-10] The increased theoretical efficiency arises from the utilization of photons below the bulk band gap: electrons are promoted from the valence band (VB) to the intermediate band (IB) and then from the IB to the conduction band (CB) by the sequential absorption of low energy photons. Incorporating an intermediate band into a functional solar cell without degrading the performance of the existing solar cell proves to be very difficult. In order to achieve an efficient IBSC the additional photocurrent generated by utilization of low energy photons in the IB must be larger than any decrease in the efficiency of the bulk junction due to the incorporation of the IB.

In order to create an efficient IBSC, several conditions must be met. Most importantly there must be enough available states in the band gap of the matrix solar cell to contribute to the photo current[11]. Ideally these available states are located at 2/3 E_g in order to utilize the largest percentage of the solar spectrum[7]. It is also important that the states in the IB be approximately half occupied in order to guarantee that there are always electrons available for promotion from the IB to the CB while ensuring that there are always vacancies in the IB that can accept electrons promoted from the VB. This can be fairly easily accomplished with doping, provided electrons are allowed to move throughout the matrix.

One of the major obstacles to realizing the IBSC device design is the suppression of Shockley-Read-Hall (SRH) recombination from the CB to the IB. SRH recombination occurs when electrons in the CB relax to lower energy states by phonon emission. One approach that has been explored for suppressing SRH recombination is to create delocalized energy bands in the IB[12-14]. The formation of delocalized states is believed to suppress SRH because the addition of one electron to a localized part of the crystal perturbs that part of the crystal, resulting in lattice vibrations in the form of phonons. A delocalized electron wave function does not perturb any particular point in the lattice and therefore couples more weakly to phonon vibrations. Consequently, delocalized intermediate bands are believed to suppress SRH recombination because the crystal would have no way of dissipating the energy lost by a relaxing electron. Suppression of SRH is one of the major driving forces for purity in materials for efficient traditional solar cells. In IBSC, however, the material introduced for the IB is inherently an impurity and can provide sites for recombination that result in a loss of useful CB electrons to the lower energy IB. As a result, it is imperative to select materials for the intermediate band that allow SRH recombination to be minimized. Finding a material that has available states at the appropriate energy levels, minimizes SRH recombination, and forms a delocalized band is a considerable challenge. One must also minimize the strain induced upon the incorporation into the matrix material, as strain based defects can also play a huge role in decreasing the efficiency of a solar cell. When considering all of these factors, InAs quantum dots in GaAs hosts have

emerged as one of the most promising materials available for an intermediate band solar cell.

Quantum dots are confined semiconductors[12]. They are confined in space by being surrounded by another higher band gap semiconductor. Consequently, an electron in a quantum dot can be promoted to a conduction band energy level, but the confinement provided by the surrounding material causes the electron to remain localized in the quantum dot. As the size of the dot is decreased below Bohr's radius, quantized energy states appear. Additional energy is then required to excite electrons to the first allowed energy state, which is above the conduction band edge. The energy separation of the quantized states, and thus the amount of additional energy required, is dependent on the degree of confinement. This confinement effect results in a tunable effective band gap that is dependent on a controllable variable (quantum dot size). This tunable band gap provides an additional degree of freedom in the design of the IB. Using this degree of freedom, it is possible to design an IB based on InAs QDs that has available states at the appropriate energy level using materials similar to the matrix solar cell (GaAs). Ideally, this results in an IB that is lattice matched and strain balanced with the matrix, thus minimizing electron recombination centers and traps.

The formation of discrete states in QDs is important to IBSC device performance. When an electron is excited into the conduction band of a bulk material, there is a continuum of available energy levels in both the conduction and valence bands. In a quantum dot, however, the addition of boundary conditions to the electron wavefunction cause it to act very differently. Constructive and destructive interference

of the wave functions allows only a few discrete energy states for the confined electron. These discrete states are useful in an IBSC because the absence of a continuum of states drastically suppresses non-radiative recombination. The continuum of bulk states makes it very easy for electrons to cascade from a high energy conduction band state to a low energy conduction band state, converting some of the energy absorbed to originally excite the electron into heat. Discrete states in confined nanostructures are separated by a significant energy difference, suppressing this relaxation process.

The IBSC model based on QD's is not without its challenges. As previously stated, a QD confines an electron three dimensionally in space. This confinement allows the IB to be tuned to the appropriate energy level and is believed to suppress nonradiative relaxation. But this same confinement makes it challenging to create the delocalized bands that are suspected to be needed to minimize Shockley-Read-Hall recombination. This challenge can be overcome, however, by taking advantage of the quantum mechanical enigma that is quantum tunneling. When two quantum dots are separated by a small (but non-negligible) barrier, there is a small probability that an electron can tunnel through the barrier from one dot to the next[13]. This probability increases as the energy levels approach resonance, reaching the limit of 1 at perfect resonance (ie: the dots have discrete states at identical energy). This results in a wave function for the electron that is delocalized over both dots[16]. This principle can be extended to an array of QD's, allowing for complete delocalization over an entire array, provided each dot in the array has identical energy levels. If the energy levels

of the quantum dots are not identical, tunneling is suppressed and the electron wavefunction is largely confined to one QD. Figure 2 shows a schematic for both an ideal QD-based IBSC and a QD-based IBSC using current growth technology.

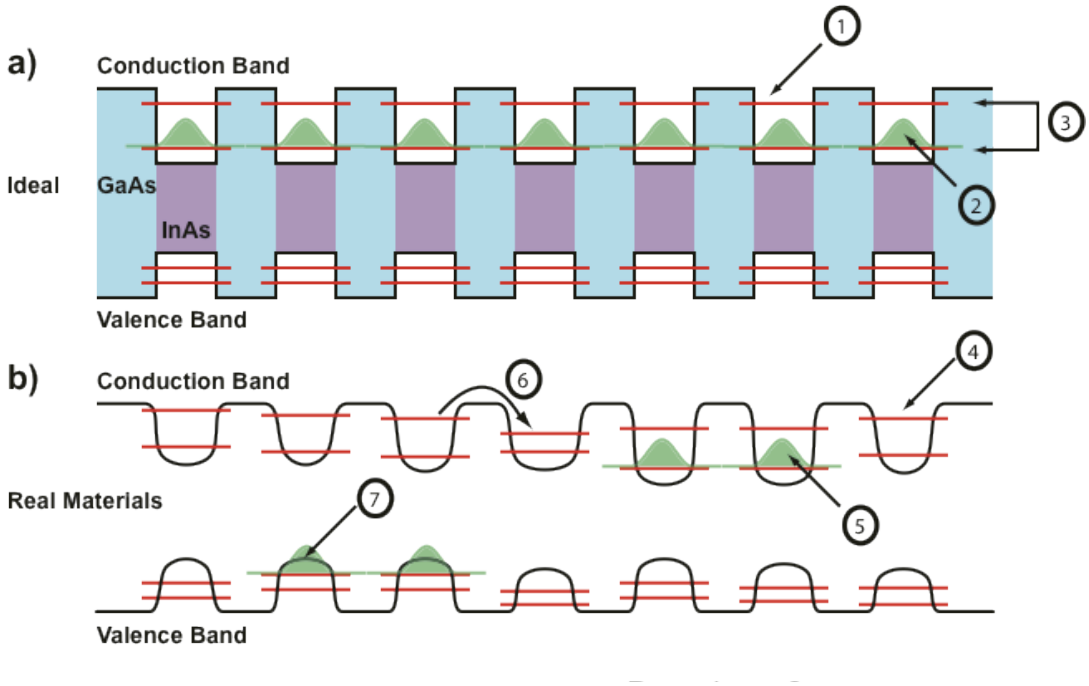

Figure 2 Schematic for real and ideal IBSC. a) Schematic band diagram of ideal IBSC with 1) identical confined energy levels in each quantum dot (red lines), 2) intermediate band with fully delocalized wavefunctions, and 3) intermediate band gaps that inhibit multi-phonon relaxation. b) Schematic band diagram of the case in real materials with 4) energy levels that vary from dot to dot, 5) localized wavefunctions, 6) potential paths for carrier relaxation by phonon emission, and 7) different spatial localization for electron and hole wavefunctions.

Despite high hopes and the dramatic increase in efficiency theoretically predicted, no IBSC device to date has demonstrated an efficiency increase resulting from the incorporation of an IB. In order to design an efficient IBSC using QD's, understanding the interactions between QDs and the formation of these delocalized states is essential. It is crucial that we understand the effect (if any) of delocalization

on the electron lifetime, and that we understand the effects of the controllable variables in the design of the system. These variables include QD size and composition, barrier thickness and composition, and distribution of energy levels.

The fundamental physics behind Intermediate Band Solar Cells suggests new opportunities to improve upon our current solar cell devices. By examining the materials parameters necessary to create an ideal intermediate band, we identify obstacles that will likely interfere with making this theoretical idea a successful reality. These obstacles, which will be identified and discussed in the next sections, have led us to revise the IBSC idea. We suggest two different types of solar cell designs that might allow for many of the benefits of an IBSC without running into the fundamental bottlenecks identified. One of the new ideas that will be discussed is a quasi-Intermediate Band Solar Cell. In this solar cell design, a QD based IBSC is created, but instead of attempting to make the intermediate band completely delocalized the QD's are organized into clusters of 3 or 4 quantum dots that allow extended states. The other idea that will be discussed is a quantum dot-based photon up-conversion solar cell device that would use quantum dots and a graded potential to convert multiple low energy photons into one high energy photon, which would then be returned to a single-junction solar cell.

Chapter 2

REALISTIC QUANTUM DOTS

Epitaxial growth allows for the most precise control of growth parameters. Epitaxially-grown QD's are not easily scalable to an industrial level and therefore are not an ideal candidate for IBSC. However, the precise control over the geometry and composition provided by this method enables systematic analysis that can reveal the fundamental photophysics and the impact of resonant tunneling. This information can then be applied to QD systems which are more economically viable, for example colloidal QD's or self-assembled nanostructures. The samples we will discuss are vertically stacked InAs QD's embedded in a GaAs matrix. The dots are grown using a technique called Stranski-Krastinov growth, which uses the lattice mismatch between InAs and GaAs to form the dot. Because the two materials have a different lattice constant, when InAs is being grown on GaAs it begins to "pile on itself" in order to minimize strain and surface energy. The InAs continues to pile on itself forming dots that can be capped by GaAs to cover and/or truncate the QDs at the desired height. The next layer of QD's is then grown on top of the previous layer, separated by the

"capping" layer of GaAs that acts as the tunneling barrier. Vertical alignment of the QDs is induced by the strain that propagates through the capping layer. In order to capture enough photons to make a difference in the photocurrent of a GaAs solar cell, approximately 50 layers of QD's will be necessary.

In theory an IBSC device would contain an array of periodically spaced identical QD's. However, inhomogeneities in the self-assembly process result in QDs that are not identical; a realistic distribution of energies has a FWHM of 0.1-1eV. Furthermore, accumulated strain becomes significant after a few QD layers and leads to structural defects. In order to alleviate strain, additional element with smaller lattice constant, (opposite of InAs, which has a larger lattice constant than GaAs), are added to the barrier layers to offset the strain induced by the InAs. This strain balancing can reduce the FWHM of the energy distribution because each layer of dot is grown under similar strain conditions, but the distribution of energy levels remains significant. The relatively thick barriers between QD's needed to accommodate strain compensation layers[11] has the additional consequence of suppressing the thermal escape of electrons by phonon assisted tunneling, as depicted in figure 3(b).

We know that resonant tunneling between QDs depends critically on the alignment of the energy levels in the two QDs and exponentially on the thickness of the barrier separating the QDs. In order to understand the impact of nanoscale structure on IBSC performance, we set out to analyze how the formation of delocalized states depends on the distribution of energy levels and the geometry and composition of the QD array. The results of the model calculation, described below,

reveal the limitations of current growth protocols for QD IBSC devices and highlight the need for a more rigorous characterization of the effect of localization on charge excitation and relaxation kinetics.

The inhomogenous distribution of QD energy levels can be seen clearly in the Gaussian distribution of QD photoluminescence energies[11]. As we will show, the inhomogeneous distribution of QD energy levels in realistic materials prevent formation of delocalized states when the QD's are separated by thick barriers. Our results quantify the improvements in QD uniformity and/or reduction in barrier thickness necessary to create spatially extended states. The results further reveal that identical QD's and delocalized states should not be assumed in realistic models of IBSC device photophysics.

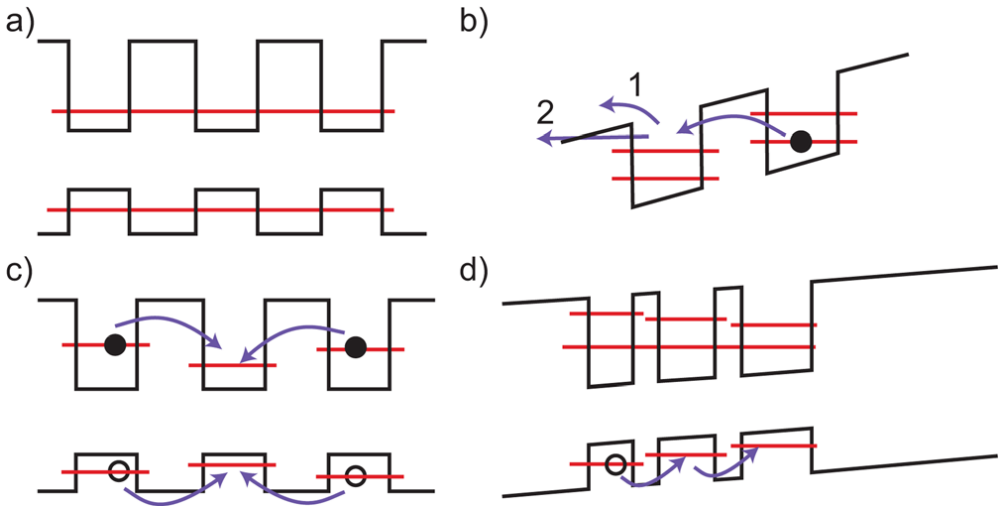

Figure 3 Schematic detailing electron transport in QD arrays. (a) schematic of delocalized bands formed an identical QD's. (b) Escape of electron from QD's in applied field via thermal (1) or tunneling (2) processes. (c) Thermalrelaxation process in arrays of closely spaced realistic QD's. (d) Delocalization over a few QD's can be achievable in a cluster of closely spaced QD's.

Chapter 3

THEORETICAL MODEL

In this model we analyze the formation of wavefunction delocalization by solving the Schroedinger equation for arrays up to 50 quantum dots with varying inhomogeneous distributions. We model the array in the growth direction as a one dimensional superlattice and capture the fluctuations in energy levels by varying the depth of the potential well for individual quantum dots. The Schroedinger equation for our system is defined as:

$$\frac{-\hbar^2}{2m^*}\frac{d^2\psi}{dx^2} + V(x)\psi(x) = \varepsilon\psi(x)$$

Where $\psi(x)$ is the wave function, ħ is plank's constant, and m^* is the electron effective mass ($0.067*m_e$ in GaAs, and $0.022*m_e$ in InAs). The potential energy profile includes the GaAs barrier heigh (0.85 eV), the barrier width (varied in the model to show the effect of barrier width), and the width of the QD potential (constant at 6.5 nm in order to have placement at the appropriate energy within the bandgap GaAs). A schematic showing the quantum dot arrangement can be seen in figure 3a.

The depth (in energy) of each QD is randomly selected within a Gaussian distribution centered on 0 with a standard deviation of σ. This replicates the consequences of random alloying and size distribution within each dot that are inevitable in the epitaxial growth process. Existing growth protocols result in energy distributions of 0.0565 eV, which we label σ_0.

We numerically solve the Schroedinger equation using Chebyshev spectral collocation methods implemented by the Chebfun Matlab package[14,15]. We calculate all wavefunctions ($\psi(x)$) composed of QD ground states by finding the n solutions of the lowest energy levels in n quantum dots. We then calculate the probability amplitude ($\psi^2(x)$) for each wave function. Figure 4(a) shows the potential profile and calculated probability amplitude for three QD's located in the middle of an array containing 30 identical QD's separated by 3nm GaAs barriers. Because the QD's are identical ($\sigma = 0$), the wavefunctions have a maximum probability amplitude that is constant over all QD's, similar to the minibands of an infinite superlattice. In figure 4(b) the QD potentials are randomly distributed within a width σ_0. As a result of the inhomogeneous distribution of energy levels, coherent tunneling is suppressed and the wavefunctions are localized in individual QD's. In figure 4(c) we plot the periodic potential and probability amplitudes for QD's separated by 10 nm barriers, which are representative of the barrier thicknesses required to accommodate strain balancing layers. Because the coherent tunneling falls off exponentially with the thickness of the barriers, the wavefunctions are localized to individual QD's despite the fact that the

width of the QD potential distribution used in the calculation of fig 2(c) is $\sigma_0/10^3$, three orders of magnitude narrower than currently achievable.

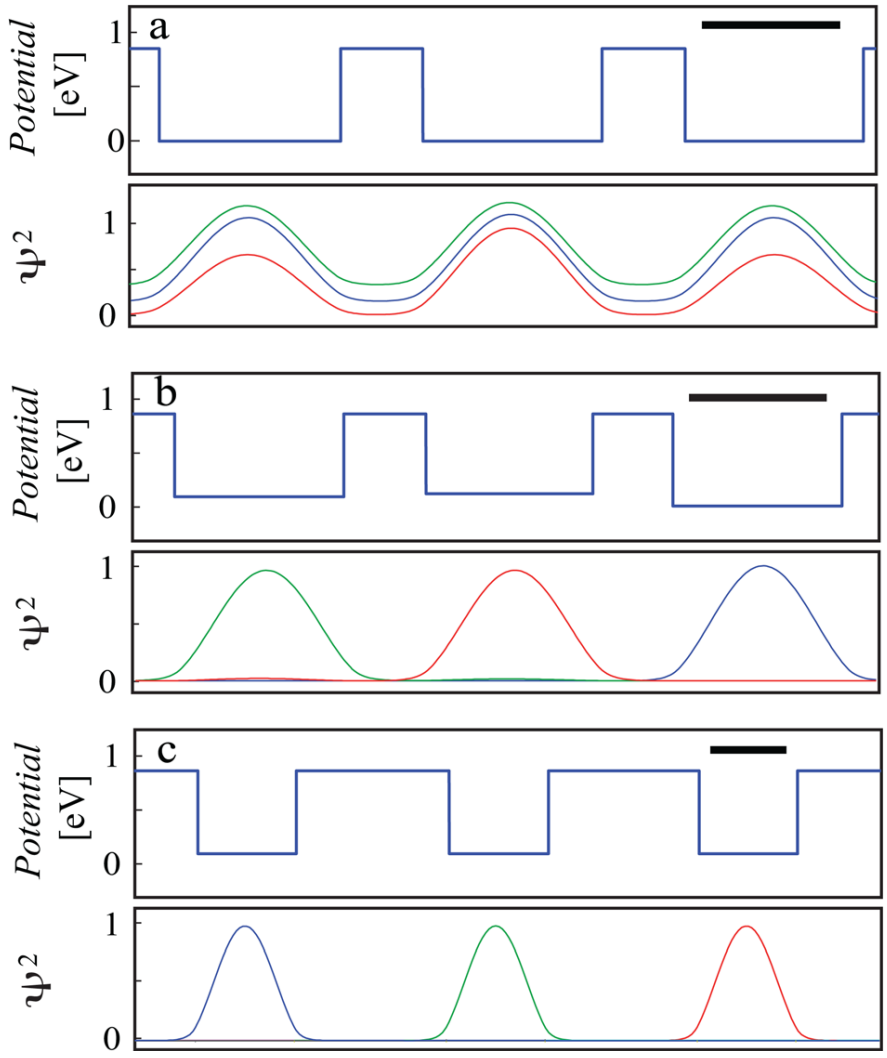

Figure 4 Wavefunctions as a function of energy distribution and barrier thickness. (a), delocalized wavefunctions in identical QD's separated by 3nm GaAs barriers, the top two curves are offset for clarity, the thick black line in all panels in 5nm long. (b) Localized wavefunctions in non-identical QD's separated by 3nm barriers with $\sigma = \sigma_0$. (c) Localized wavefunctions in non-identical QD's separated by 10nm barriers with $\sigma=\sigma_0/10^3$.

The calcualation presented in figure 4 demonstrates that arrays of realistic QD's separated by barriers as small as 3nm must be viewed as a series of localized states. The existence of localized states must induce deviations from the rates of optical excitation and nonradiative relaxation predicted for delocalized bands[16]. The localized states also create pathways for phonon assisted tunneling that funnel multiple carriers to a single QD (Fig. 3(c)), increasing the probability of thermal relaxation.

Figure 4 qualitatively demonstrates the difficulties of forming delocalized wavefunctions with current growth methods and shows how this becomes even more difficult at the increased barrier thicknesses necessary to mitigate strain. In order to quantitatively describe wave function delocalization we must go one step further. We assess the uniformity of QD energy levels necessary to achieve delocalized bands by calculating the average spatial extent of wavefunctions (the average localization length, ξ) as a function of σ. To determine ξ we first determine the QD on which each wavefunction is centered (ie: the location of the maximum of each $\psi^2(x)$. We then calculate the number of QD's that contain a wavefunction amplitude of at least 10% cut-off amplitude. We repeat all calculations using a 1% cut-off amplitude to assess the impact of this cut-off value on the resulting analysis. We independently calculate ξ for all n ground state wavefunctions in a single realization of the random potential profile of n QD's. We then repeat the process for 5 separate realizations of the random QD potential. The average and standard deviation of ξ is calculated using all the wavefunctions in all random realizations that have the same σ and QD separation.

In figure 5(a) we plot ξ vs σ for QD's separated by 10 nm and 3 nm barriers using both a 10% (open symbols) and 1% (closed symbols) cut-off amplitude. ξ is presented in units of the number of QD's over which the wavefunction is extended. When QD's are separated by 10 nm barriers (diamonds) we find that the delocalized states are not formed until σ drops below $\sigma_0/10^4$. Wave functions delocalized over nearly 50 QD's do not occur until energy distributions approach $\sigma_0/10^5$. When the barrier thickness is reduced to 3 nm (circles), the increased tunneling strength due to thinner barriers allows for delocalization over several QD's when $\sigma=\sigma_0/10$. Wavefunctions delocalized over nearly 50 QD's do not occur until energy distributions approach $\sigma_0/10^2$. We find that considering a 1% cut-off fraction (closed symbols) relaxes the σ requirement to form delocalized states by a factor of about 2 for both the 3 and 10 nm cases. Consequently we conclude that the exact value of the cut-off amplitude does not impact our overall result: when QD's are separated by barriers of 3 nm or more, the formation of wavefunctions delocalized over nearly 50 QD's requires a distribution of QD energy levels at least 2 orders of magnitude narrower than produced by current growth methods.

Although there are techniques for narrowing the QD energy level distribution, including annealing and growing on pre-patterned substrates, improving uniformity by 2 to 5 orders of magnitude is an extraordinary and likely insurmountable challenge because the self-assembly of InAs QD's involves diffusion, which is inherently random. We therefore analyze the separation of QD's necessary to create delocalized states with realistic distributions of QD energy levels. In figure 5(b) we plot the

average localization length as a function of barrier thickness. The results reveal that electron wavefunctions delocalized over at least 5 QD's can be achieved when the QD's are separated by barriers of 1.5 nm or less.

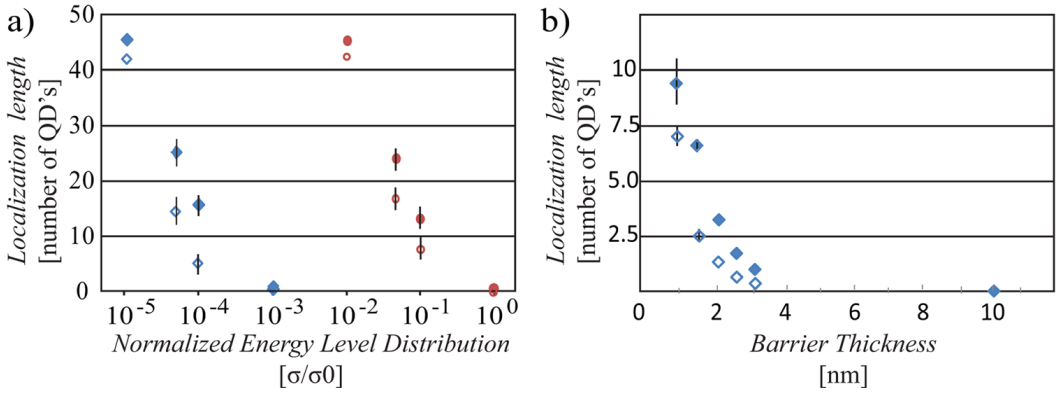

Figure 5 Localization as a function of energy distribution and barrier thickness. (a) Localization length plotted as a function of σ for 50 QD's separated by 3nm barriers (circles) and 10 nm barriers (diamonds). The spatial extent is calculated using both a 10% (open) and 1% (solid) cut-off for the probability amplitude. (b) Localization length plotted as a function of barrier thickness for presently achievable values of the QD homogeneity (σ_0)

Present models of IBSC devices suggest that fully delocalized IB states are ideal. However, as shown through the previous theoretical examination of the system, it is clear that the Intermediate "Band" is far from being truly delocalized. Furthermore achieving a truly delocalized intermediate band may prove to be impossible using current fabrication techniques.

The new information illuminated by the model described above makes it clear that we must at the very least change the way we think about the intermediate band in IBSC, because we clearly do not have delocalized bands in our current IBSC devices. Although assumed to be important at reducing recombination into the intermediate band, it is not clear precisely how much a delocalized intermediate band would

improve the quality of a device, and experimental data demonstrating the electron lifetime dependence on delocalized, semi-localized, and localized wavefunctions will be needed in order to answer this question (an experiment to reveal this question is currently in progress and will be discussed in detail on pages 13 and 14). It is possible that a fully delocalized band is not needed to significantly impact the rates. If the electron lifetime were to change significantly when the wavefunction was delocalized over only two or three quantum dots, it may be possible to design variations on the Intermediate Band Solar Cell that could achieve significant efficiency improvements by organizing the quantum dots into small clusters of three or four closely spaced quantum dots over which the electrons would be delocalized. These clusters could be separated by relatively large spacer layers that permit relief of the strain accumulation within the cluster. This may allow for the utilization of delocalization without requiring massive improvements in the precision of our growth techniques.

The cluster idea allows for small amounts of wavefunction delocalization by decreasing the barrier thickness between clusters. Also, it can somewhat mitigate strain build-up by engineering the thick barrier layers between clusters to compensate for strain build-up. However it is not clear how many QD's would be needed in each cluster to reduce nonradiative relaxation into the dots, and it is quite possible that this number would exceed the limits that allow for strain mitigation. Only experiments demonstrating the electron lifetime dependence on localization will answer this question. If the decrease in relaxation from the conduction band to the intermediate band due to delocalization is significant enough to outweigh the losses due to the

incorporation of an intermediate band, then a cluster-based IBSC could likely produce highly efficient solar cells that outperform their single-junction counterparts.

Chapter 4

QUANTUM DOT BASED PHOTON UP-CONVERSION

This brings us to another idea, called photon up-conversion, which could still use nanostructure engineering to utilize low-energy photons. This approach uses low-energy photons in a way that does not depend on wavefunction delocalization in a QD array. Furthermore, the photon up-conversion idea does not introduce strain or defects in the main solar cell. The idea of photon up-conversion is depicted in Figure 6 on the following page.

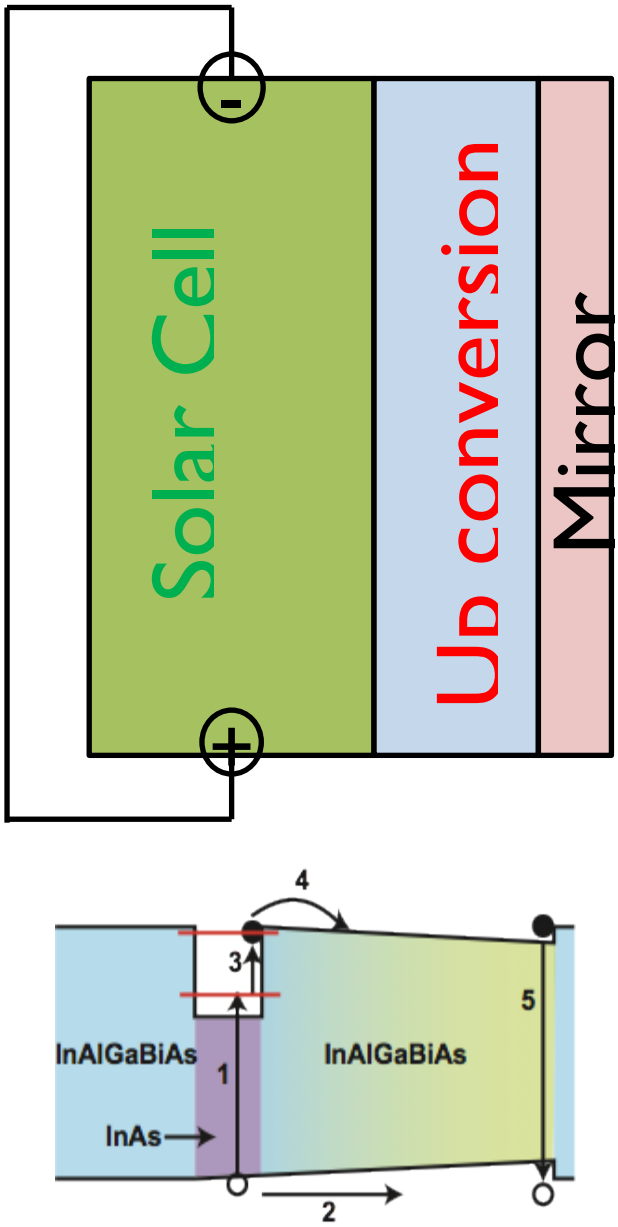

Figure 6 Photon up-conversion schematic. (top) depiction of the geometry for a photon up-conversion device, (bottom) more detailed schematic of photon up-conversion process. (1) Low energy photons that pass through the InAlGaBiAs solar cell excite an electron in the InAs QD. (2) The hole is stripped away by the use of a graded potential engineered using InAlGaBiAs in order to decrease the likelihood of recombination in the QD. (3) A second low energy photons promotes the electron from the lowest energy electron state in the QD to a higher energy confined state. (4) The electron tunnels out of the excited QD state via electron tunneling through a triangle barrier. (5) The electron recombines with the hole in the InAlGaBiAs, releasing a photon with energy equal to 1 + 3 - (Energy lost in graded potential).

The photon up-conversion idea utilizes a two-photon process within the QD in order to make use of low energy photons that would usually be lost. What makes this idea different from the IBSC idea is that the quantum dots are positioned *after* a single-junction solar cell as opposed to within the solar cell. Because of this, simply promoting the electrons directly to the higher energy conduction band is not enough to harvest current from low energy photons, as there is no electrical connection between the solar cell and the up-conversion device. Instead, the two photon process is used to promote the electron within the up-conversion nanostructure before it is allowed to recombine with the optically-generated hole to emit a photon that is sent back to the working solar cell (processes 1, 3, and 5 respectively in figure 6). A graded potential is needed to strip the hole away during the first low-energy photon excitement to decrease the probability of radiative recombination from the ground state in the QD, which would not emit a photon of sufficient energy to excite an electron in the solar cell. The excited energy state in the conduction band of the quantum dot needs to be designed to be towards the top of the confining potential. If this is done, a second low-energy photon excites an electron from the ground state of the QD to the excited QD state, permitting the electron to tunnel through the small triangular tunneling barrier that exists at the top of the well adjacent to the graded potential (process 4). Once this is accomplished, the electron will recombine with the hole created and moved by processes 1 and 2. This will result in a photon with energy slightly less than the two photons used to excite the electron to the excited state in the QD conduction band. This concept may have advantages over the IBSC idea because it allows for the use of

low energy photons via the two photon absorption process without introducing intermediate states within the solar cell. The wide band gap solar cell can be engineered to have maximum efficiency with little to no defects. Separate from the solar cell we can use QD's to convert low energy photons into useful high-energy photons.

The important engineering questions in this up-conversion idea all deal with the rates of excitation, relaxation and tunneling. These are many of the same rates that need to be considered to shed light on the IBSC/IBSC cluster questions regarding electron lifetime. It is crucial that process 2 (the stripping of the hole from the QD) happens faster than the radiative recombination between the ground state electron and hole. This should be easily accomplished by the graded potential in the valence band of the QD (assuming zero or close to zero valence band offset can be achieved), because the graded potential will move the hole on picosecond time scales whereas radiative recombination occurs on the nanosecond time scale. The more important rate competition comes after the electron is promoted from the ground state of the QD to the excited state (process 3). At this point the electron tunneling process (process 4) must occur faster than the relaxation from the excited state back to the ground state. The relaxation process occurs very quickly, and therefore the energy levels and tunneling barriers must be precisely engineered in order to allow the electron tunneling to compete with this process.

The question regarding natural radiative lifetime between an electron and hole in the ground state (the process competing with process 2 on the diagram), can be

modeled by examining the wavefunction overlap between the electron and hole using the following equation.

$$\frac{1}{\tau_{rad}} = \frac{2\pi n E^2 f}{3em_0\lambda_c}$$

Where τ_{rad} is the radiative lifetime, E is the energy difference between the electron and hole, and f is the oscillator strength (essentially the amount of overlap between the electron and hole wave functions). The oscillator strength is highly dependent on electric field, but for electric fields typical in a p-n junction in a GaAs solar cell, the radiative lifetime is typically on the order of 1 nanosecond.

Figure 7 below shows a depiction of the electron and hole wavefunctions under zero and finite electric fields. Reduced wave function overlap increases the lifetime of the exciton. This lifetime and its dependence on electric field can be directly investigated using time-resolved photoluminescence. The methods of TRPL will be described in the next section and preliminary results will be compared to the model.

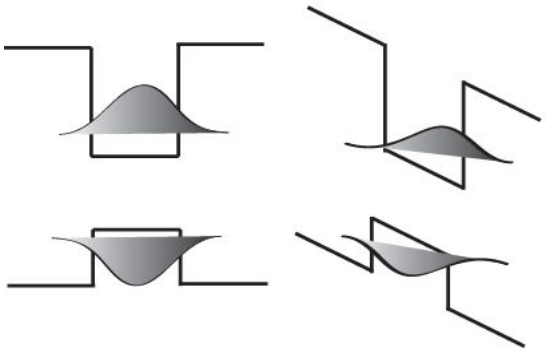

Figure 7 Wavefunction overlap as a function of electric field. Shows the wavefunction overlap between (left) electron and hole in a QD with 0 net field, and (right) electron and hole in a QD with non-zero electric field.

The tunneling from the higher energy state can be modeled as a function of electric field or extent of the graded potential. The tunneling rate, Γ, is a function of the barrier height (W), the slope of the potential (F), and the distance necessary to travel through the barrier to reach an open state of equivelant energy (L). The tunneling rate can be described by the following equation

$$\Gamma = \frac{\hbar\pi}{2m^{*}L} * \exp\left(\frac{4\sqrt{2m^{*}W^{3}}}{3\hbar F}\right)$$

As is made evident by the above equation, in order to decrease the tunneling time one must minimize the tunneling barrier. This requires engineering the excited state in the QD to be as close to the top of the confining potential as possible. If one were to make the graded potential steeper, one could also decrease the tunneling time but this would result in a more significant loss of energy of the electron, thus decreasing the energy of the subsequent high energy photon created by recombination between electron and hole.

Chapter 5

EXPERIMENTAL

The previous sections have discussed several semiconductor nanostructures based on quantum dots that could enable harvesting of more of the solar spectrum. The rates of electron relaxation and escape from these nanostructures are critical device parameters. A deeper understanding of the connection between nanoscale structure and charge dynamics is necessary to design nanostructures that maximize efficiency in these types of device.

In order to understand the dependence of charge escape and relaxation dynamics on nanoscale structure and composition, it is important to be able to tune the barrier and the potential of a QD in-situ. Equally important is the ability to control the coupling between QDs and explore the consequences of the formation of delocalized states. As discussed earlier, ensembles of QDs have a distribution of energy levels that make the QDs non-identical. Consequently, ensemble measurements lose the precise control of energy levels and delocalization that we need. We investigate the charge carrier dynamics in single quantum dots and explore how these rates change when one

QD is coupled to another. We do this with a model system that includes two QDs separated by a thin tunnel barrier. Due to the growth constraints discussed earlier, it is very unlikely the two dots will start out in resonance with each other. Electrons and holes are therefore localized in individual QDs in the as-grown structures. To create delocalized states we need to tune the energy levels of the two dots independently. When an electric field is applied to a stacked pair of QD's, the energy levels of the dots change. The effect of field on the energy of recombination is dependent on the particular state. States in which the electron and hole are localized within the same dot are only affected by the quantum-confined stark effect. States with the electron and hole in different dots are not only affected by QCSE but also by the interaction of the electron-hole pair with the electric field. The effect of field on the energy of an exciton scales with the distance separating the electron and hole, and therefore is much greater for an electron-hole state in which the electron and hole are spatially separated in two different dots than when the electron and hole are localized within the same QD. Because these two states are affected differently by field, it is possible to tune these two states into resonance with each other. At the specific electric field where the energy of an electron-hole pair localized in the same dot is equal to that of the energy of an electron-hole pair separated in different dots, the two states are degenerate. This degeneracy results in a delocalized electron that is shared between the two states[20-22]. By examining the electron lifetimes of the two states as they are tuned in and out of resonance, one can learn valuable information concerning the rates of excitation and relaxation and how they change as the electron becomes more and more delocalized.

We measure the rates of electron relaxation using time resolved photoluminescence. In a normal photoluminescence (PL) experiment, the sample is optically excited in order to measure the energy of the photons emitted after electron-hole recombination. PL spectra contain information about the confined energy states of electrons and holes and the coulomb interactions between the charges. Because the states available for electrons in a QD are discrete, they can easily be identified and independently examined. In order to isolate a single pair of QD's, a patterned mask is placed over a sample containing coupled, dispersed QD's grown by the Stranski-Krastinov growth method described earlier. The density of dots on the sample is chosen so that ~ 1 pair of QD's will be within the 1 micron apertures on the pattern, allowing for the measurement of single QDs or QD pairs. Electrodes are connected to apply a voltage from the bottom to the top of the sample in order to allow for tuning of the energy levels. The QD sample is placed in a closed cycle cryostat which cools the sample to 10 K. The extremely cold temperatures are necessary in order to suppress phonon vibrations in the lattice, which act as an uncontrolled source of electron excitation or relaxation.

In order to controllably excite electrons in the coupled QD's, a Ti:Saphire laser is used. The laser outputs pulses of light with a width of ~150 femtoseconds spaced by 13 ns and with tunable wavelengths from 700 to > 900 nm. The power of the laser can be controlled externally. The laser is directed towards the sample and focused using an objective microscope. This produces a spot size on the micron scale. Each pulse from the laser promotes electrons from the VB to the CB, and these electrons eventually

relax to the ground state, emitting a photon. These photons are directed towards a 0.75 m Princeton Instruments Acton spectrometer. The spectrometer spatially separates light of different wavelengths before directing it towards a liquid nitrogen cooled charge coupled device (CCD). The CCD measures the intensity of light of different wavelengths by "counting" the number of photons that hit a particular pixel. The peaks in the resulting spectrum result from specific energy levels in the quantum dots under the aperture being examined. The spectrum can be taken as a function of excitation wavelength, excitation power, and electric field. All of these parameters are crucial in determining the physical origin of each spectral line (ie: which state in the system do they arise from). After identifying an aperture that contains the signatures of coupling, the specific spectral lines can be selected for further experimentation concerning the time dependence of the electron relaxation.

As stated before, a spectrometer spatially separates light of different wavelengths. This is important because it enables us not only to measure the energy of the light emitted from the sample, but also to select specific portions of the emitted light in order to attain information on a specific QD state, specifically information concerning the lifetime of an excited electron. In order to measure the lifetime, the desired wavelength of emitted PL is directed through a narrow slit on the side of the spectrometer and on to an avalanche photodiode (APD). The APD is sensitive to the arrival of single photons. The avalanche photodiode works in parallel with a trigger diode to determine the exciton lifetime. In short, a pulse from the laser is split, with one portion directed towards a trigger diode that starts a clock. The rest of the laser

excitation pulse is directed towards the sample where electron-hole pairs in the QD under observation are excited. Electrons eventually recombine with the holes, resulting in emission of a photon with energy equal to the energy lost by the electron and hole due to recombination (i.e. a photon energy that correlates to specific discrete energy states). Photons with wavelengths of interest are directed out of the spectrometer to the APD, which stops the clock. The process is repeated with the next pulse. It is important that the delay between pulses (in this case 13 ns) be significantly longer than the lifetimes of interest (in this case picoseconds to ~5 ns)[20,21]; this allows for all of the physics of relaxation to be examined before the next pulse arrives.

The experimental set-up described above allows for the examination of single pairs of QD's. See figure 6 below for a schematic and brief description of the components in experimental set up. Both the lifetime of an excited electron-hole pair and the energy of the discrete states in the QD's can be measured. Most importantly, they can be measured as a function of electric field, which can be used to tune the pair of dots in and out of resonance. This allows for a fundamental study to be performed, characterizing the effect of delocalization.

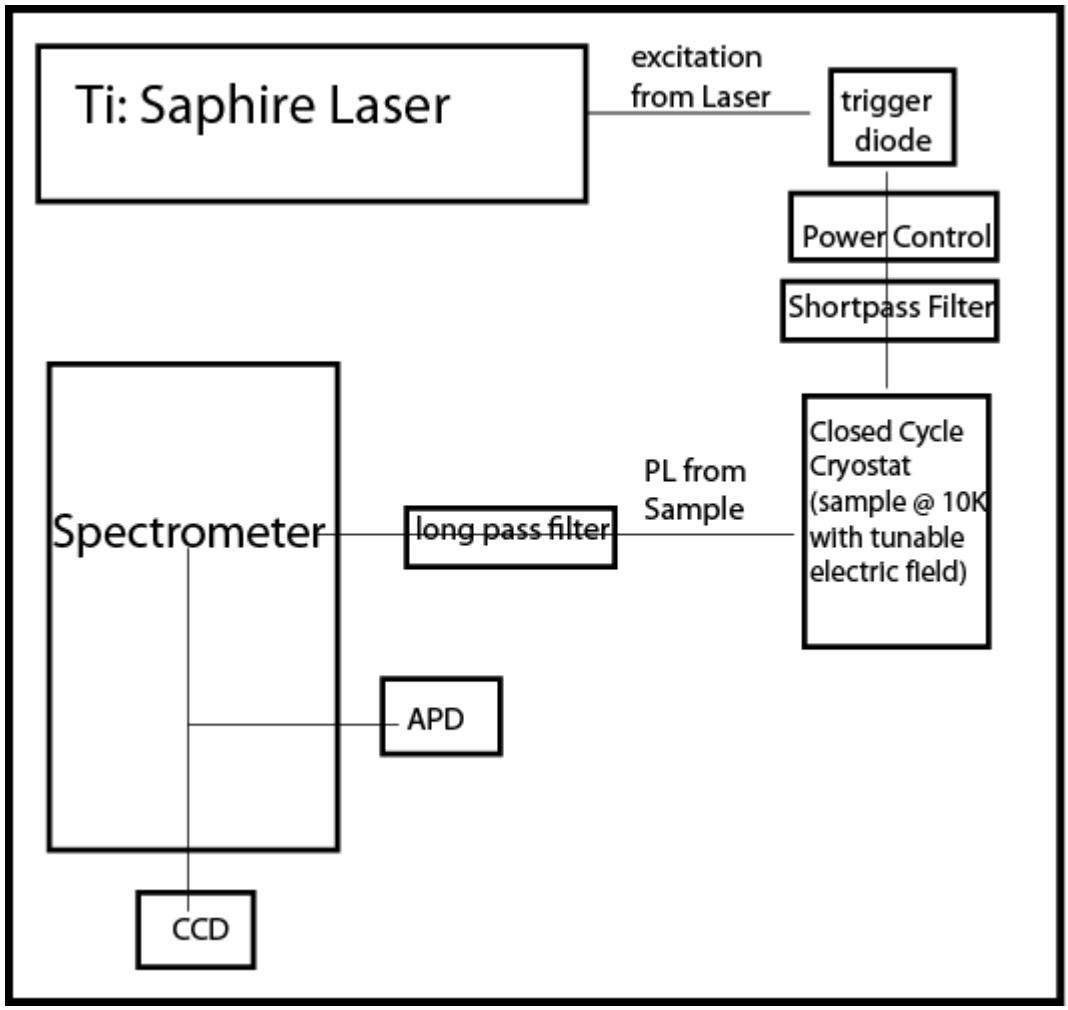

Figure 8 Time Resolved Photoluminescence experimental setup shows the overall layout of the experiment. The pulsed output from the laser excites the trigger diode, starting the clock. The laser wavelength and power is then controlled so that the conditions of excitation are controlled. The excited sample emits photons to the spectrometer. Wetting layer light and reflected laser light are filtered out using long pass filters. The light is spatially separated according to wavelength by the spectrometer and sent to the CCD. After using the CCD to identify the states of interest, light of a specific wavelength can be directed toward the APD to stop the clock.

Chapter 6

DATA AND ANALYSIS

The experimental procedure described above was used to study a sample containing vertically stacked coupled QD's separated by a very small (2 nm) barrier. An aperture showing evidence of coupling was excited using an 880 nm laser beam. See Appendix 1 for details of the analysis leading to the conclusion that there was evidence of coupling. The bias map and time correlated data for areas where there is evidence of resonant tunneling (and therefore delocalization) can be seen in figure 7 below.

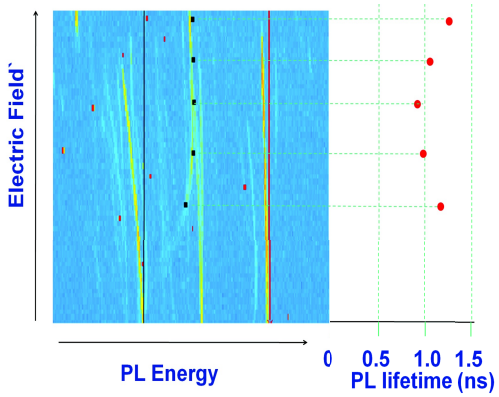

Figure 9 TRPL bias map. shows the field dependent lifetime of an electron state that shows signs of coupling with the neighboring state. The sample was excited with an 880 nm pulsed laser; the field was altered in steps of 0.01 V per 45 seconds; the signal is approximately 7 counts per second above the noise.

The lifetime values are obtained by deconvolving the data with the instrument response function of the APD and determining the exponential decay constant that best fits the remaining data.This process, as well as examples of the raw data, is described in more detail in Appendix 2. The figure above suggests that there is a change in the lifetime of the electron at or near resonance, which likely originates in wavenfuction delocalization. The data, while encouraging, is not yet sufficient to understand the connection between materials structure, quantized states and charge carrier dynamics. Additional data is needed to allow a systematic investigation of this connection and propose rate equation models that explain the data.

Chapter 7

FUTURE WORKS

To extend the work presented here, theoretical models predicting electron lifetimes as a function of field need to be completed and compared to data collected on single quantum dots. In order to connect the fundamental physics of a two-QD system to the IBSC theory, examples of the electron lifetime dependence on coupling will be needed from a multitude of different samples. Multiple examples of coupled QD's with different geometries (most importantly barrier layer) need to be attained. Samples of vertically stacked QD's with 2 nm, 3 nm, 4 nm and 6 nm barriers are readily available and need to be examined.

In addition to adding to the quantity of data and attaining data as a function of barrier thickness, I also feel there is an opportunity to better understand the data. The time resolved data is a result of billions of excitations and consequent emissions. Emitted photons are not perfectly collected, so often only ~ 200 emitted photons per second are collected by the APD. Each data point tells the lifetime of that particular electron. Collecting emitted photons over many cycles allows for reconstruction of the

PL decay curve. Embedded in the decay curve are all of the physical processes that contributed to the decay curve. As described in more detail in appendix 2, it is difficult to pull out the physical processes that contribute to the overall decay curve. When analyzing this problem it is obvious that the excited electron in the QD can undergo multiple different processes that all result in the emission of a photon at the same energy. For example, electrons excited above the energy state of interest could non-radiatively relax to the state of interest before emitting a photon, adding another component to its lifetime other than purely that of an electron excited directly into the state of interest. Each of these processes can be described by its own decay constant that contributes to the overall lifetime. For the data attained above (figure 7) this was largely ignored, and only the overall lifetime was considered. However, it may be possible to attain more information about the different rates at play by taking power dependent data. Non-radiative relaxation into the state of interest and excitation out of the state of interest are both processes that can contribute to the overall lifetime and therefore can be described by their own decay constant. Both of these processes are also very dependent on power and excitation wavelength. It is therefore likely possible to gain valuable information about these processes by performing studies of a particular state that are dependent on both power and excitation wavelength.

Chapter 8

CONCLUSIONS

Quantum Dots have unique properties that make them a powerful engineering tool that can be utilized to capture and manipulate light. They can theoretically be used in intermediate band solar cells where they can enhance efficiencies by approximately 50%. However, we have shown that growth and fabrication techniques do not yet allow for the type of precision necessary for the QD-based device to perform as predicted. As shown in Chapter 4, an increase of three orders of magnitude in the homogeneity of quantum dot energy levels is needed to create an array capable of satisfying the assumptions of existing theoretical models. This result illustrates a disconnect between the theory and reality of delocalized states in intermediate bands formed from QDs. Recognizing this disconnect, we have proposed two different ideas to utilize quantum dots in solar cell devices. The first is the cluster-based intermediate band solar cell, in which clusters of quantum dots are used to make many mini-intermediate bands in which delocalized states are achievable. The second idea proposed is a quantum dot-based photon up-conversion solar cell, in which the

combination of a quantum dot and a graded potential can be used in tandem in order to convert two low-energy photons into one high energy photon.

In order to develop effective quantum dot-based solar cell devices it is important to analyze the fundamental physics that are at play when light is absorbed and excites electrons in a quantum dot. We must then explore how the structure and composition of the QD and surrounding materials impacts the dynamics of charge carrier relaxation in order to identify ways in which the structure can be engineered to enhance efficiency. In the two ideas described above, as well as in the traditional IBSC solar cell design, the crucial fundamental rates needed to accurately describe the system dynamics are the same. All that is necessary is an understanding of the electron lifetime as a function of electric field (in order to determine the tunneling rate), the amount of localization/delocalization, and (for the up-conversion idea specifically) the non-radiative relaxation rate from a high energy quantum dot state to a lower one. We have described methods for obtaining much of this information using time-resolved photoluminescence and present preliminary results obtained with this method.

REFERENCES

1. "World Energy Demand and Economic Outlook." *International Energy Outlook 2010*. 2 January , 2011. Unite States Energy Information Administration . Web. 02 March 2011. <http://www.eia.doe.gov/oiaf/ieo/world.html>.
2. Thomas Friedman (2008). *Hot, Flat, and Crowded*. Farrar, Straus and Giroux, New York. ISBN 978-0-374-16685-4.
3. "Overview*" About NREL*. 26 January 2011. National Renewable Energy Laboratory. Web. 02 March 2011. <http://www.nrel.gov/overview/ >
4. *Basic Research Needs for Solar Energy Utilization*: *Report on the basic Energy Sciences Workshop on Solar Energy Utilization.* 25 June 2005. Web. 02 March 2011. p 22. *<http://www.sc.doe.gov/bes/reports/files/SEU_rpt.pdf >*
5. "Solar Research" *Science and Technology*. 26 January 2011. National Renewable Energy Laboratory. Web. 02 March 2011. <http://www.nrel.gov/solar/
6. W. Shockley and H. J. Queisser, "Detailed Balance Limit of Efficiency of p-n Junction Solar Cells," *Journal of Applied Physics,* vol. 32, pp. 510-519, 1961.

7. A. Luque and A. Martí, "Increasing the efficiency ofIdeal solar cells by photon induced transitions at intermediate levels," *Physical Review Letters,* vol. 78, pp. 5014–5017, 1997

8. A. Martí, L. Cuadra, and A. Luque, "Design constraints ofthe quantum-dot intermediate band solar cell," *Physica E,* vol. 14, pp. 150--157, 2002.

9. G. L. Araujo, A. Marti, Solar Energy Mater. Solar Cells 1994, 33, 213.

10. A. Luque, A. Marti, C. Stanley, N. Lopez, L. Cuadra, D. Zhou, J. L. Pearson, and A. McKee, "General equivalent circuit for intermediate band devices: Potentials, currents and electroluminescence," *Journal of Applied Physics,* vol. 96, pp. 903-909, 2004.

11. V. Popescu, G. Bester, M. C. Hanna, A. G. Norman, and A. Zunger, "Theoretical and experimental examination of the intermediate-band concept for strain-balanced (In,Ga)As/Ga(As,P) quantum dot solar cells," *Phys. Rev. B,* vol. 78, p. 205321, 2008..

12. C. Tablero, A. Martí, D. F. Marrón, E. Antolín, and A. Luque, "Intermediate bands and non radiative recombination," *Proc. of the 23th European Photovoltaic Solar EnergyConference (Valencia),* pp. 403-406, 2008

13. A. Martí, E. Antolín, E. Cánovas, N. López, P. G.Linares, A. Luque, C. R. Stanley, and C. D. Farmer, "Elementsof the design and analysis of quantum-dot intermediate band solar cells," *Thin Solid Films,* vol. 516, 2008.

14. T. Drscoll, F. Bornemann and L. Trefethen, BIT Numer, Math. 48, 701, 2008.

15. A. Birkisson and T. Driscoll, “Automatic Frechet Differentiation for the numverical solution of boundary value problems,” ACM Trans. Math Softw. (submitted).

16. S. Tomic. Phys Rev. B 82 195321 (2010)

17. A. Martí, L. Cuadra, and A. Luque, "Quasi driftdiffusion model for the quantum dot intermediate band solar cell," *IEEE Transactions on Electron Devices,* vol. 49, pp. 1632–1639, 2002.

18. Davies, John. *The Physics of Low Dimensional Semiconductors: An Introduction.* Cambridge University Press. Cambridge, U.K. 1998.

19. R**.** de L. Kronig and W. G. Penney, in *Proc. Roy***.** Soc., vol. A130**,** p.499. 1930

20. A.S. Bracker, M. Scheibner, M.F. Doty, E.A. Stinaff, I.V. Ponomarev, J.C. Kim, L.J.Whitman, T.L. Reinecke, D. Gammon. *Engineering electron and hole tunneling with asymmetric InAs quantum dot molecules.* Appl. Phys. Lett. **89**, 233110 (2006)

21. M. Scheibner, I.V. Ponomarev, E.A. Stinaff, M.F. Doty, A.S. Bracker,C.S. Hellberg, T.L. Reinecke, D. Gammon. *Photoluminescence spectroscopy of the molecular biexciton in vertically stacked InAs-GaAs quantum dot pairs.* Phys. Rev. Lett. **99** 197402 (2007).

22. M.E. Ware, E.A Stinaff, D. Gammon, M.F. Doty, A.S. Bracker, D. Gershoni, V.L. Korenev, S.C. Badescu, Y. Lyanda-Geller, T.L. Reinecke. *Polarized fine structure in the photoluminescence excitation spectrum*

of a negatively charged quantum dot. Phys. Rev. Lett. **95** 177403 (2005).

Appendix A

UNDERSTANDING THE SPECTRA

Because the samples contain randomly distributed QD's, each aperture is not certain to contain a pair of coupled QD's. Some apertures will have no dots underneath, resulting in a spectrum with no peaks (i.e. purely noise). Other apertures contain a multitude of dots underneath, resulting in a spectrum with many discrete peaks that can be difficult to understand. One of the most important aspects of this PL experiment is being able to understand the spectra in order to optimize the experimental conditions to increase the signal to noise ratio.

The most critical aspect of the experimental process is electric field. If the sample is in the wrong bias range, the band structure can tip, causing the electrons to flood out of the dots into the surrounding material and virtually eliminating any photon emission from the QDs. By running a simple IV curve of the sample, we can determine the electric field that results in a band structure that prevents this flooding

Once the appropriate bias range is established, the different apertures can be scanned in the bias range that allows for the electron and hole states of the QD to be examined. This results in spectra containing discrete peaks. Each peak represents a

different state of the system underneath the aperture, but as stated before it is not clear immediately what the peaks represent. Three key variables can be tuned to help understand what the different peaks represent: excitation wavelength, excitation power, and electric field.

Multiple peaks in the figure above can be a result of any combination of multiple energy levels from multiple dots. By seeing how the spectra changes with excitation wavelength, we can begin to interpret what the different peaks represent. There is a direct correlation between the excitation wavelength and the photon energy. Higher energy photons have the ability to excite electrons to a higher potential. This can be useful when trying to maximize the number of photons emitting from the dots when scanning apertures to find the appropriate focal spot to examine. Often a wavelength capable of exciting in the wetting layer, where there is a band of available states, is chosen initially. At the appropriate electric fields, band tipping dictates that the electrons excited in the wetting layer tunnel into the discrete states of the dot where they will recombine. This results in peaks from multiple states inside the underlying QD (or QD's) and the increased availability of excited electrons results in an increase in emitted photons. The increased number of photons emitted from the sample aides in the optimization of the focusing objective. Once the optimization process is complete, the wavelength is increased above 870 nm in order to excite directly in the dot, rather than in the wetting layer). This results in an overall decrease in the intensities of the peaks, which is disproportionately distributed so that the higher energy peaks resulting from second and third harmonics in the dot(s) decrease much

more than the ground states. As the wavelength is increased, the higher energy states disappear into the noise of the spectrum leaving behind the lowest energy states. This information allows for the identification of the ground states represented in the spectrum and from there we can begin to identify any other important spectral lines.

As a compliment to the information learned by decreasing the excitation wavelength, one can learn valuable information by tuning the excitation power. Whereas excitation wavelength directly correlates to the energy of the photons used for excitation, excitation power directly correlates to the number of photons available for excitation. An increased number of photons increases the likelihood for multiple photon processes, and therefore increases the intensity of charged exciton and biexciton states. Even at high excitation wavelength, peaks resulting from the recombination of higher energy states can be significantly above the noise, provided there are enough photons around to allow for sequential photon absorption. Decreasing the power further decreases the likelihood of higher energy states being present in the spectrum. If multiple peaks remain after decreasing the power (normally to < 5 mW for our experimental set-up) and increasing the excitation wavelength (to around 900), it is likely that the remaining peaks result from ground state recombination from multiple QD's.

Once the dependence on wavelength and power is determined, the coupling between the remaining states (if any) can be determined by changing the electric field. Electric field has multiple effects on a confined system. As stated in paragraph 2 of this appendix, electric field tips the band structure of confined systems, which can

greatly influence the charging of the dot and the dynamics of the charged dot. Another result of applying electric field to a confined system is the quantum confined Stark effect (QCSE). The QCSE is most simply described as the separation of electrons and holes in response to electric field. Because electrons and holes have opposite charge, they are naturally affected differently by electric field. However, in a confined system where the charges have no place to go they essentially pile up on opposite sides of the quantum dot, altering the energy of recombination. This is a similar physical consequence of electric field to the one described in the experimental section previously, in which the recombination energy of an electron hole pair delocalized among multiple dots is affected by electric field due to the spatial separation of the charges. For QCSE within a single QD however, the effect is quite small. This effect can make it difficult to determine if changes in the energy of spectral lines as a result of applied electric field are due to QCSE or coupling between dots. Taking a bias map that shows the response of the system to a wide variety of fields illustrates any coupling between spectral lines and allows for the distinction between the two.

Bias maps of coupled QD's can contain many interesting signatures. For instance, the signature energy shift between an exciton (an electron-hole pair) and a negative trion (a state including two electrons and one hole) is typically 6 meV. Charging of states when the electric field crosses the Fermi level set by the doping also results in distinct shifts in the spectral. All of this information helps to identify the distinct states that correspond to specific spectral features.

Appendix B

TIME CORRELATED DATA

The time correlated data acquired using the method described in the experimental section is a result of the accumulation of billions of data points. Represented by that data are multiple different processes that the electron could undergo before finally recombining and emitting a photon. The final result can best be described as an exponential decay.

The decay constant of the exponential decay curve that best describes the data is related to the average lifetime of an excited electron before recombining and emitting a photon at the wavelength in question for a particular electric field.

$$Intensity(t) = A_{avg}e^{(-t/\tau_{avg})}$$

A_{avg} relates to the intensity of the peak and is largely dependent on the signal to noise ratio of the peak in question; τ_{avg}represents the average lifetime of the sample. In principle, the equation should be written as a sum of exponentials with the time constant for each exponential corresponding to different physical loss pathways. Increasing the number of exponentials increases the degrees of freedom for the fitting

process and typically results in somewhat better fits to the data. The improved fit, however, does not guarantee that the increased number of free parameters will have any particular physical meaning. In order to understand whether there is physical meaning to additional time constants, data must be collected as a function of variables that change dynamics of a particular state. For example, excitation wavelength and power significantly change the dynamics, and the expected trends for the rates of secondary loss pathways are largely known. Without this additional data, it is largely impossible to confidently deconvolve anything beyond a single exponential average lifetime. With this additional data it may be possible to better understand the kinetics of charge carrier transport and loss in these nanostructures.